

# Magnetic field sensing beyond the standard quantum limit using 10-spin NOON states

Jonathan A. Jones,<sup>1</sup> Steven D. Karlen,<sup>2</sup> Joe Fitzsimons,<sup>2,3</sup> Arzhang Ardavan,<sup>1</sup>  
Simon C. Benjamin,<sup>2</sup> G. A. D. Briggs,<sup>2</sup> and John J. L. Morton<sup>1,2,\*</sup>

<sup>1</sup>CAESR, Clarendon Laboratory, Oxford University, Oxford OX1 3PU, United Kingdom

<sup>2</sup>Department of Materials, Oxford University, Oxford OX1 3PH, United Kingdom

<sup>3</sup>Institute of Quantum Computing, University of Waterloo, Waterloo, ON, N2L 3G1, Canada  
(Dated: June 19, 2022)

The concept of entanglement, in which coherent quantum states become inextricably correlated [1], has evolved from one of the most startling and controversial outcomes of quantum mechanics to the enabling principle of emerging technologies such as quantum computation [2] and quantum sensors [3, 4]. The use of entangled particles in measurement permits the transcendence of the standard quantum limit in sensitivity, which scales as  $\sqrt{N}$  for  $N$  particles, to the Heisenberg limit, which scales as  $N$ . This approach has been applied to optical interferometry using entangled photons [5, 6, 7] and spin pairs for the measurement of magnetic fields and improvements on atomic clocks [8]. Here, we demonstrate experimentally an 9.4-fold increase in sensitivity to an external magnetic field of a 10-spin entangled state, compared with an isolated spin, using nuclear spins in a highly symmetric molecule. This approach scales in a favourable way compared to systems where qubit loss is prevalent, and paves the way for enhanced precision in magnetic field sensing.

A single spin will precess in the presence of a magnetic field. In the rotating frame used to describe magnetic resonance, this precession occurs at a rate governed by the detuning  $\delta$  of the magnetic field from resonance (expressed in frequency units), such that the state  $|0\rangle + |1\rangle$  evolves as  $|0\rangle + e^{i\delta t}|1\rangle$  (for clarity, normalisation constants are omitted throughout). This principle forms the basis of several kinds of magnetic field sensor, where the externally applied field  $\delta$  is detected as a phase shift. States possessing many-qubit entanglement can acquire phase at a greater rate and thus offer an enhanced sensitivity to the applied field.

The requirements for constructing the resource of a large number of entangled spins are less severe than those for a complete NMR quantum computer [9, 10, 11]. Indeed, rather than striving towards individual addressability of each constituent nuclear spin, an element of indistinguishability is instead advantageous in quickly and efficiently growing the state. For example, we consider here a star topology with one central spin,  $A$ , and  $N$  peripheral  $B$  spins which cannot be separately addressed (see Figure 1A)).

Although the  $B$  spins, in separate spatial modes, must be formally distinguishable, they cannot be distinguished by any NMR observable and their behaviour is well described by number states, as used to describe photon

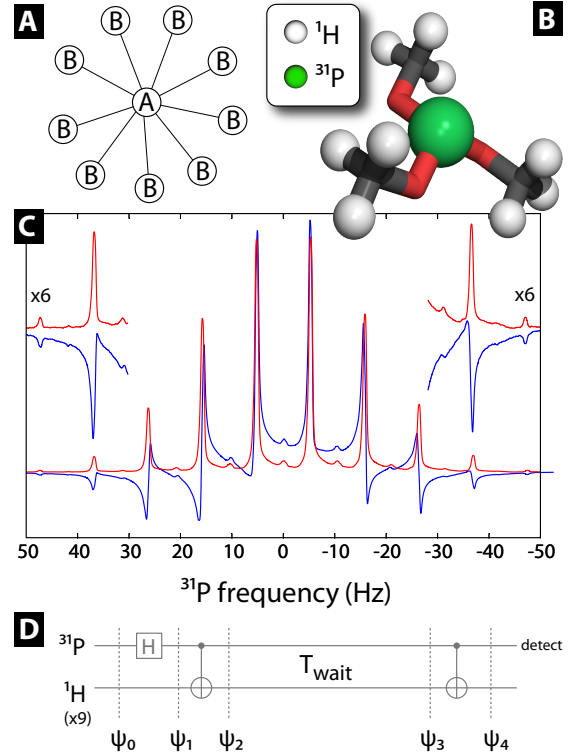


**FIG. 1: 10-spin NOON states are created using nuclear spins in the TMP molecule** (A) Topology of the spin qubits used to generate the spin-NOON state. (B) The trimethyl phosphite (TMP) molecule consists of a central  $^{31}\text{P}$  nuclear spin surrounded by nine identical  $^1\text{H}$  spins. (C) The initial  $^{31}\text{P}$  NMR spectrum of TMP (red). Nuclear spin-NOON and MSSM states are generated and allowed to evolve for some short time under the influence of an off-resonance magnetic field. After mapping these entangled states back to the  $^{31}\text{P}$ , the resulting spectrum (blue) shows how the phase shift acquired increases with the lopsidedness of the state. Low-intensity peaks between pairs of NMR lines arise from coupling to  $^{13}\text{C}$  impurities. (D) Spin-NOON states are generated by first applying a Hadamard gate to the  $^{31}\text{P}$  followed by a controlled-NOT on the nine equivalent  $^1\text{H}$ .

occupation in one of two modes. Many-body entanglement in such states has been referred to by the epithet NOON state [12, 13], and has received much attention for its ability to offer quantum-enhanced sensitivity in optical interferometry. We define the spin-NOON state as  $|\psi_{\text{NOON}}\rangle = |N_{\downarrow}, 0_{\uparrow}\rangle + |0_{\downarrow}, N_{\uparrow}\rangle$ , a superposition of the

$N$  spins being all down, and all up (this has also been described as a ‘‘Schrödinger cat’’ state, being the superposition of the two most distinct states [14]). Such a spin-NOON state will acquire phase  $e^{iN\delta t}$  thus showing an  $N$ -fold increase in the phase accrued for a given  $\delta$ , and hence a greater sensitivity to the applied field.

Through single spin-flips, the spin-NOON state may be transformed to what we term ‘many,some + some,many’, or MSSM, states. For example, the state  $|01000\rangle + |10111\rangle$  is one of the five possible  $|\psi_{4114}\rangle$  states. For the purposes of this study, it is convenient to classify these states by the difference in the Hamming weight of the two elements of the superposition, or its lopsidedness  $\ell$  (i.e.  $|\psi_{pqqp}\rangle$  has  $\ell = |p - q|$ ). In the general case, spins  $A$  and  $B$  have different sensitivities to the applied field, and so the enhancement in magnetic field sensitivity of the total system depends on a weighted form of  $\ell$ , which we call  $\ell_\gamma$ , which includes the relative gyromagnetic ratios of the  $A$  and  $B$  spins.

A molecule with a suitable star topology is trimethyl phosphite (TMP), illustrated in Figure 1B, comprising one central  $^{31}\text{P}$  spin and nine identical surrounding  $^1\text{H}$  spins (the intervening O and C nuclei are mostly spin-zero and may be neglected). The NMR spectrum of  $^{31}\text{P}$  is shown in Figure 1C (red curve). Coupling to the local  $^1\text{H}$  spins shifts the resonance frequency of the  $^{31}\text{P}$  by some amount depending on the total magnetisation of the  $^1\text{H}$ . Within the pseudo-pure state model [9, 10, 11], the lines in the  $^{31}\text{P}$  NMR spectrum can thus be assigned to the following  $^1\text{H}$  states:  $|9, 0\rangle, \rho_{8,1}, \rho_{7,2}, \dots, \rho_{1,8}, |0, 9\rangle$ . Any experimentally accessible MS state is an equal mixture of the relevant pure states  $|M, S\rangle_i$ , where  $i$  runs over the microscopic (and indistinguishable) permutations of  $|M, S\rangle$ . Thus, for clarity we describe MS states in terms of the density matrix  $\rho_{M,S} = \sum_i |M, S\rangle_i \langle M, S|_i$ .

Given the gyromagnetic ratios of  $^1\text{H}$  and  $^{31}\text{P}$  (42.577 and 17.251 MHz/T, respectively), one would predict a  $\sim 23$ -fold enhancement in phase sensitivity of the 10-spin NOON state over a single  $^{31}\text{P}$  nucleus, or a factor of  $\sim 9.4$  enhancement over the single  $^1\text{H}$  nucleus most commonly used in current sensors.

The  $A$  spin ( $^{31}\text{P}$ ) in the star topology is distinguishable, and its state is therefore given separately in the spin basis. Following Figure 1D, we assume that all spins start in a ground state:  $\Psi_0 = |0\rangle_A |000\dots 0\rangle_B = |0\rangle |N, 0\rangle$ . A Hadamard gate is applied to  $A$ , followed by a C-NOT gate applied to the  $B$  spins, controlled by the state of  $A$ , yielding  $\Psi_2 = |0\rangle |N, 0\rangle + |1\rangle |0, N\rangle$ : an  $(N + 1)$ -spin NOON state with the relevant lopsidedness  $\ell_\gamma = (N\gamma_B + \gamma_A)/\gamma_B$ . After some period  $T_{\text{wait}}$ ,  $\Psi_3 = |0\rangle |N, 0\rangle + e^{(i\ell_\gamma \delta T_{\text{wait}})} |1\rangle |0, N\rangle$ . A second identical C-NOT is applied to the  $B$  spin to map the total phase acquired onto  $A$ :  $\Psi_4 = (|0\rangle + e^{(i\ell_\gamma \delta T_{\text{wait}})} |1\rangle) |N, 0\rangle$  which is directly detected. A similar method has been used to create a 1+3 spin entangled state for the purposes of enhanced spin detection [15].

Rather than relying on pseudo-pure state preparation, we can select to observe the evolution of one of the 10 NMR lines and thus effectively post-select the signature of a particular initial state, analogous to the way in which post-selection has been employed in linear optics experiments on NOON states [7]. By applying the entangling operation described above and observing the line corresponding to the original  $B$  ( $^1\text{H}$ ) state  $|9, 0\rangle$  we can identify the 10-spin NOON state  $|0\rangle |9, 0\rangle + |1\rangle |0, 9\rangle$  and discern its behaviour in the presence of a magnetic field detuning  $\delta$ .

Figure 1C (blue curve) shows a measurement of  $^{31}\text{P}$  obtained after the pulse sequence described above and shown in Figure 1D. The free evolution time,  $T_{\text{wait}}$ , was set to 400  $\mu\text{s}$  such that given the magnetic field detuning ( $\sim 3.13 \mu\text{T}$ ) a phase shift of  $\sim 0.107\pi$  would be experienced by a single  $^1\text{H}$  spin. Observing the left-most line ( $\sim 48 \text{ Hz}$ ) is equivalent to post-selecting the  $|0\rangle |9, 0\rangle$  initial state, and thus the 10-spin NOON state with  $\ell_\gamma = 9.4$ , which has instead acquired a  $\sim \pi$  phase shift during the free evolution period. Repeating the experiment with  $T_{\text{wait}} = 0$  yields a spectrum identical to the original NMR spectrum, neglecting dephasing and small changes in the impurity lines.

An advantage of the mixed initial state of the  $^1\text{H}$  nuclei is that it allows us to simultaneously probe the evolution not just of the  $\ell_\gamma = 9.4$  pseudo-pure NOON state described above, but all MSSM states for this spin system ( $\ell_\gamma = |9.4 - 2m|$  where  $1 \geq m \geq 9$ ). For example, the line at  $\sim 37 \text{ Hz}$  corresponds to the  $\rho_{8,1}$  initial state of the  $B$  spins which, under the operations applied, will yield the MSSM state  $\rho_{8118}$  with  $\ell_\gamma = 7.4$ , where we define

$$\rho_{MSSM} = \sum_i (|0\rangle |M, S\rangle_i + |1\rangle |S, M\rangle_i) \otimes (\langle 0| \langle M, S|_i + \langle 1| \langle S, M|_i). \quad (1)$$

Although observing at this frequency corresponds to selecting the mixture  $\rho_{8118}$ , each element of the mixture acquires phase at the same rate, and a phase shift of  $\sim 0.79\pi$  is observed. The phase acquired is less than for the ( $\ell_\gamma = 9.4$ ) state, but the signal-to-noise is much greater, arising from the larger number of spins in the appropriate initial state. This illustrates the fact that in the limit of high temperature, where spin polarisation is weak, one of the intermediate MSSM states with  $\ell < N + 1$  can yield the optimum sensitivity to magnetic field offset.

To explore the evolution of the many-body entangled states in more detail, the evolution time  $T_{\text{wait}}$  was varied. As  $T_{\text{wait}}$  increases, the signal from each line undergoes oscillations whose frequency varies with  $\ell_\gamma$ . Figure 2 shows the Fourier transform with respect to  $T_{\text{wait}}$ , measured for the 10 different lines in the  $^{31}\text{P}$  NMR spectrum. The frequency, which corresponds to a sensitivity to the magnetic field detuning, increases as one moves to the outer lines of the spectrum, corresponding to MSSM states

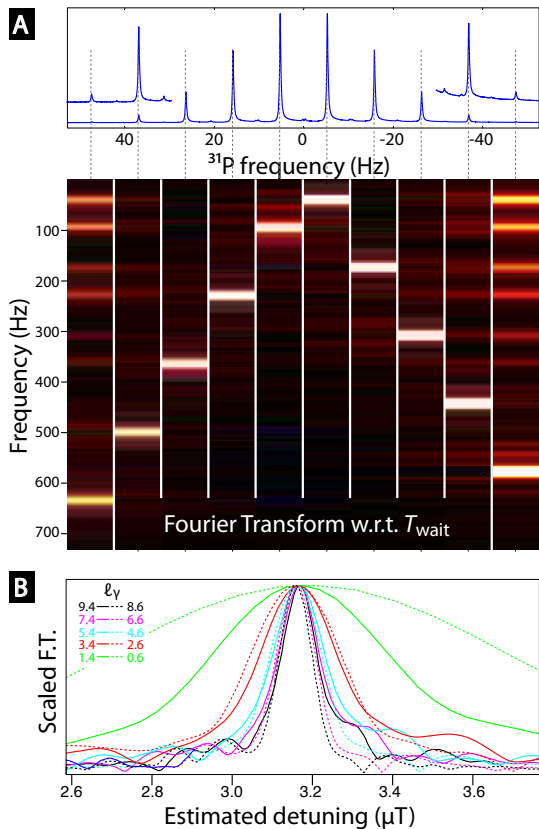


FIG. 2: **Nuclear spin-NOON states demonstrate an entanglement-enhanced sensitivity to an external magnetic field.** (A) The Fourier transform of the evolution of each of the 10 NMR lines with respect to  $T_{\text{wait}}$  (see Figure 1D) shows an increasing frequency proportional to the increasing lopsidedness  $\ell_\gamma$  of the entangled state produced. The intensity has been normalised using the intensities of the initial spectrum — the residual asymmetry in intensities is an artifact of static field inhomogeneity. The  $^{31}\text{P}$  NMR spectrum of the TMP molecule is shown above for reference. (B) The Fourier transform peak allows an estimate of the effective magnetic detuning from resonance of the  $^1\text{H}$  spins, which improves with the use of higher- $\ell$  states. Solid and dashed lines represent NMR lines to the left and right of centre, respectively. All peaks are scaled to unit intensity.

with larger  $\ell$ , to a maximum for the spin-NOON states at the ends. The linewidth similarly increases slightly due to enhanced decoherence of the states with larger  $\ell$ , however, this increase is sub-linear [16] and so when the precession frequency is used to extract an estimate of magnetic field detuning, the uncertainty falls as states with larger  $\ell$  are used (Figure 2B).

The states which we exploit are of the general kind referred to as ‘cat states’, after the famous thought experiment of Erwin Schrödinger[1]. Our  $|\psi_{\text{NOON}}\rangle$  is a simple cat state of size  $N = 10$  particles. A state of the form  $\rho_{MSSM}$  is more complex, but we may say that it is *equivalent* to a canonical cat state which decoheres at

the same rate [17, 18]. Then, despite being a mixture,  $\rho_{MSSM}$  is nevertheless classified as a cat state of full size  $N$  within the local decoherence model of Ref [17] (since neither the bit flips nor the mixing inherent in  $\rho_{MSSM}$ , alter the rate at which locally independent phases accumulate). If instead we have global decoherence sources then the effective cat size will correspond to the lopsidedness  $|M - S|$ , for precisely the reasons of field sensitivity described above.

While both optical and spin-based NOON states offer Heisenberg limited sensitivity in the absence of errors, the latter can be fundamentally more robust in real scenarios. Photon loss can be crippling in linear optical systems: Losing even a single photon from a NOON state prevents the phase build up from being measured. As the number of photons in the NOON state is increased, the probability of obtaining a successful measurement result decreases exponentially. The sensitivity of the NOON state scales only linearly with its size, so the decreasing probability of success rapidly removes any advantage gained through the use of entanglement. For a fixed probability of photon loss,  $\epsilon$ , this imposes a fundamental limit, corresponding to the minimum of the dashed curves in Figure 3. The optimum size of an optical NOON state scales as  $-\log(1 - \epsilon)^{-1}$ , beyond which the use of larger entangled states is detrimental to sensitivity.

Molecular spin-NOON states do not suffer loss in the same manner as optical systems, and the dominant source of error becomes dephasing noise caused by unaccounted for fields experienced by individual spins. We can characterise the effect of such noise versus increasing system size using an appropriate measurement strategy. In a noise-free system, the rate at which phase  $\phi$  is acquired by the spin-NOON state would correspond directly to the field strength to be detected. We wish to minimise the variance in this quantity, i.e.

$$\Delta^2 \left( \frac{\partial \phi}{\partial t} \right) = \frac{\Delta^2 \phi}{t^2} = \frac{1}{N^2 t^2}. \quad (2)$$

where the second equality follows from Ref. [13]. Given a fixed time  $T_{\text{tot}}$  to perform the sensor operation, one could opt to make  $M$  separate measurements each of exposure time  $T_E = T_{\text{tot}}/M - T_G$ , where  $T_G$  is the gating and measurement time. This strategy will minimise the effects of finite local noise, provided that  $T_G \ll T_E$ . The variance on the mean of  $M$  individual measurements is

$$\begin{aligned} \Delta^2 \delta &= \frac{1}{M} \left( \frac{1}{N^2 T_E^2} + \frac{1}{N^2} \sum_{i=1}^N \Delta^2 h_i \right) \\ &\approx \frac{1}{T_{\text{tot}}} \left( \frac{1}{N^2 T_E} + \frac{T_E}{N} \Delta^2 h \right), \end{aligned} \quad (3)$$

where  $h_i$  is the phase contribution to spin  $i$  from local fields. For any non-zero  $\Delta^2 h$ , minimising this quantity will yield  $T_E \propto N^{-1/2}$ , resulting in  $\Delta^2 \phi \propto N^{-3/2}$ . The

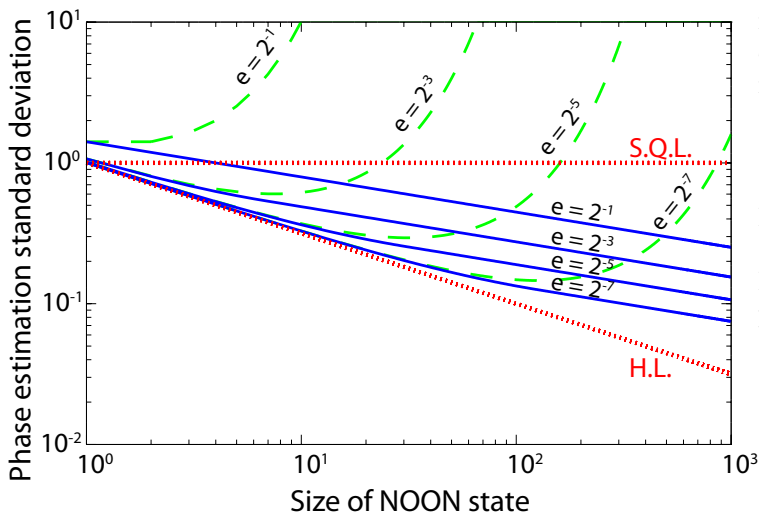


FIG. 3: **Spin-NOON states exhibit an enhanced robustness to noise over optical NOON states.** A comparison of the effect of noise on the standard deviation of phase estimates for spin-NOON (blue solid curves) and optical NOON states (green dashed curves) for a range of error probabilities. For photonic systems, the dominant source of error is taken to be photon loss, which is assumed to occur with probability  $\varepsilon$ . For spin-NOON states the dominant source of error is taken to be a set of random normally distributed magnetic fields which lead to complete dephasing of disentangled spins with probability  $\varepsilon$  over the timescale of the measurement. The upper and lower dotted lines indicate the standard quantum limit and the Heisenberg limit respectively. The contribution is plotted per spin/photon, rather than per NOON state, in order to allow a direct comparison of states of varying size.

sensitivity of the system thus limits to  $N^{3/4}$ : logarithmically midway between the standard quantum limit and the Heisenberg limit. Provided that the measurements can be made on a time scale short compared to the decoherence time of the spin-NOON state ( $\propto N^{-1/2}$ ), creating larger entangled states will produce greater sensitivity, in contrast to the case for photonic systems.

In addition to demonstrating how an enhanced sensitivity to magnetic fields can be achieved using entanglement in nuclear spins, this work represents progress towards the realisation of ‘spin amplification’ schemes which use a bath of  $B$  spins to measure the state of  $A$  for the purposes of single spin detection [15]. Analogous to the way in which photon loss poses a limitation to the extent of the resource (photon number) which can be called up for entanglement-enhanced measurement, a weak thermal polarisation will limit the effectiveness of this scheme for practical magnetometry. Fortunately, the approach described here is readily applicable to electron spins, which can offer a high degree of polarisation at experimentally accessible magnetic fields and temperatures. Furthermore, dynamic nuclear polarisation, which is already employed in several methods for mag-

netic field sensing using nuclear spins [19], or algorithmic cooling [20, 21], could be applied here to yield improvements over currently achievable sensitivity.

This research is supported by the EPSRC through the QIP IRC [www.qipirc.org](http://www.qipirc.org) (GR/S82176/01) and CAESR (EP/D048559/1). J.F. is supported by Merton College, Oxford. G.A.D.B. is supported by the EPSRC (GR/S15808/01). J.J.L.M. acknowledges St. John’s College, Oxford. J.J.L.M., S.C.B and A.A. acknowledge support from the Royal Society.

## METHODS

The sample was a 1:1 by volume solution of trimethylphosphite and acetone- $d_6$ , degassed using freeze-pump-thaw cycles, and flame sealed in a 5 mm NMR tube. All NMR experiments were performed on a Varian INOVA 600 spectrometer using a  $^{31}\text{P}$  probe with a  $^1\text{H}$  decoupler coil and  $^2\text{H}$  lock at a temperature of  $20^\circ\text{C}$ .  $\pi/2$  pulse lengths were approximately  $30\ \mu\text{s}$  on both channels, and the spin-spin coupling  $^3J_{\text{PH}}$  was 10.5 Hz. Measured  $^{31}\text{P}$  relaxation times were  $T_2 = 2.2\ \text{s}$  and  $T_1 = 5.6\ \text{s}$ , while  $^1\text{H}$  relaxation times were  $T_2 = 2.3\ \text{s}$  and  $T_1 = 12.5\ \text{s}$ .

C-NOT gates were implemented using standard NMR techniques [11] with two  $^1\text{H}$   $\pi/2$  pulses separated by a spin echo of length  $1/2J$ , where  $J$  is the spin-spin coupling constant. All pulses were implemented as BB1 composite pulses [22] to reduce the effects of RF inhomogeneity.

\* Electronic address: [john.morton@materials.ox.ac.uk](mailto:john.morton@materials.ox.ac.uk)

- [1] Schrödinger, E. Discussion of probability relations between separated systems. *Proceedings of the Cambridge Philosophical Society* **31**, 555–563 (1935).
- [2] Deutsch, D. Quantum theory, the Church-Turing principle and the universal quantum computer. *Phil. Trans. R. Soc. A* **400**, 97 (1985).
- [3] Yurke, B. Input states for enhancement of fermion interferometer sensitivity. *Phys. Rev. Lett.* **56**, 1515–1517 (1986).
- [4] Giovannetti, V., Lloyd, S. & Maccone, L. Quantum-enhanced measurements: Beating the standard quantum limit. *Science* **306**, 1330–1336 (2004).
- [5] Leibfried, D. *et al.* Creation of a six-atom ‘Schrödinger cat’ state. *Nature* **438**, 639–642 (2005).
- [6] Roos, C. F., Chwalla, M., Kim, K., Riebe, M. & Blatt, R. ‘Designer atoms’ for quantum metrology. *Nature* **443**, 316–319 (2006).
- [7] Nagata, T., Okamoto, R., O’Brien, J. L., Sasaki, K. & Takeuchi, S. Beating the standard quantum limit with four-entangled photons. *Science* **316**, 726–729 (2007).
- [8] Meyer, V. *et al.* Experimental demonstration of entanglement-enhanced rotation angle estimation using trapped ions. *Phys. Rev. Lett.* **86**, 5870–5873 (2001).

- [9] Cory, D. G., Price, M. D. & Havel, T. F. Nuclear magnetic resonance spectroscopy: An experimentally accessible paradigm for quantum computing. *Physica D* **120**, 82–101 (1998).
- [10] Gershenfeld, N. A. & Chuang, I. L. Bulk spin-resonance quantum computation. *Science* **275**, 350 (1997).
- [11] Jones, J. A. NMR quantum computation. *Prog. NMR Spectrosc.* **38**, 325–360 (2001).
- [12] Sanders, B. C. Quantum dynamics of the nonlinear rotator and the effects of continual spin measurement. *Phys. Rev. A* **40**, 2417–2427 (1989).
- [13] Lee, H., Kok, P. & Dowling, J. A quantum Rosetta stone for interferometry. *J. Mod. Opt.* **49**, 2325–2338 (2002).
- [14] Knill, E., Laflamme, R., Martinez, R. & Tseng, C. H. An algorithmic benchmark for quantum information processing. *Nature* **404**, 368–370 (2000).
- [15] Cappellaro, P. *et al.* Entanglement assisted metrology. *Phys. Rev. Lett.* **94**, 020502 (2005).
- [16] Krojanski, H. G. & Suter, D. Scaling of decoherence in wide NMR quantum registers. *Phys. Rev. Lett.* **93**, 090501 (2004).
- [17] Dür, W., Simon, C. & Cirac, J. I. Effective size of certain macroscopic quantum superpositions. *Phys. Rev. Lett.* **89**, 210402 (2002).
- [18] Note that the second approach of Ref. [17], that based on distillation, does not immediately generalise from their pure states to our mixed states: Under the constraint of single qubit operations one cannot “produce – with unit probability –  $n$ -party GHZ states” for  $n > 1$ .
- [19] Kernevez, N. & Glénat, H. Description of a high sensitivity CW scalar DNP-NMR magnetometer. *IEEE trans. on Mag.* **27**, 5402–5404 (1991).
- [20] Baugh, J., Moussa, O., Ryan, C. A., Nayak, A. & Laflamme, R. Experimental implementation of heat-bath algorithmic cooling using solid-state nuclear magnetic resonance. *Nature* **438**, 470–473 (2005).
- [21] Ryan, C. A., Moussa, O., Baugh, J. & Laflamme, R. Spin based heat engine: Demonstration of multiple rounds of algorithmic cooling. *Phys. Rev. Lett.* **100**, 140501 (2008).
- [22] Cummins, H. K., Llewellyn, G. & Jones, J. A. Tackling systematic errors in quantum logic gates with composite rotations. *Phys. Rev. A* **67** (2003).